Radiocarbon, Vol 00, Nr 00, 2021, p 1–16 DOI:10.1017/RDC.2021.78

DO RADIOCARBON AGES OF PLANT WAX BIOMARKERS AGREE WITH ^{14}C-TOC/ OSL-BASED AGE MODELS IN AN ARID HIGH-ALTITUDE LAKE SYSTEM?

Bernhard Aichner[1]* • Merle Gierga[2] • Alexander Stolz[3] • Monika Mętrak[4] • Mateusz Wilk[4] • Małgorzata Suska-Malawska[4] • Steffen Mischke[5] • Dirk Sachse[6] • Ilhomjon Rajabov[7] • Nasimjon Rajabov[7] • Janet Rethemeyer[3]

[1]Dept. of Ecosystem Research, Institute of Freshwater Ecology and Inland Fisheries (IGB), Müggelseedamm 301, 12587 Berlin, Germany
[2]Institute of Geology and Mineralogy, University of Cologne, Zülpicher Str. 49B, 50674 Cologne, Germany
[3]Institute of Nuclear Physics, University of Cologne, Zülpicher Str. 77, 50937 Cologne, Germany
[4]Faculty of Biology, Biological and Chemical Research Centre, University of Warsaw, Żwirki i Wigury 101, 02-089 Warsaw, Poland
[5]Institute of Earth Sciences, University of Iceland, Sturlugata 7, 102 Reykjavík, Iceland
[6]GFZ German Research Centre for Geosciences, Section 4.6 Geomorphology, Organic Surface Geochemistry Lab, 14473 Potsdam, Germany
[7]Climate Change and Ozone Center, State Administration for Hydrometeorology of the Republic of Tajikistan, 47 Shevchenko Street, 734025 Dushanbe, Tajikistan

ABSTRACT. To elucidate the dynamics of terrestrial leaf waxes in a high-altitude lake system, we performed compound-specific radiocarbon analysis (CSRA) of long-chain *n*-alkanes in two sediment core sections from Lake Karakul (Pamirs, Tajikistan) and in surface soil samples from the catchment area. We aimed to answer the question whether the *n*-alkanes are delivered into the lake sediment with substantial delay due to storage in soils, which may cause a potential bias when used as paleoenvironmental proxies. In the surface soils, the CSRA results reveal an age range of *n*-alkanes from modern to 2278 ± 155 cal BP. In the two sediment core samples, three of the four *n*-alkane ages fell on the lower ends of the 1σ-uncertainty ranges of modeled ages of the sediments (based on AMS ^{14}C-TOC and OSL dating results). We conclude that sedimentary leaf waxes represent compounds with intermediate turnover time in soils, for example originating from alluvial plains close to the shores. Overall, the results provide evidence that sedimentary leaf wax compounds in this cold and arid setting are potentially older than the conventional age model indicates, but these findings need to be interpreted in context of the generally large uncertainty ranges of such age models.

KEYWORDS: chronology, compound-specific radiocarbon analysis, leaf waxes, *n*-alkanes, Pamirs, Central Asia.

INTRODUCTION

Sediment cores are commonly used as climate archives, whose proxy-data interpretation relies on age-depth models. In particular, proxies need to represent the time of deposition, but significant lag times potentially occur on the riverine to marine pathways and in large lake catchment areas before a climate signal is deposited into sediments (Eglinton et al. 1997). A proxy group which is especially prone to such lag times is terrestrial organic biomarkers, e.g., long-chain *n*-alkanes derived from leafs and roots of terrestrial plants, which are frequently used as hydroclimatic indicators (Eglinton and Hamilton 1967; Castañeda and Schouten 2011). This is mainly because of significant residence time in soils due to high recalcitrance of compounds, their transport via rivers, as well as mixing processes, resuspension, and redistribution of material from floodplains from which it was reworked after a long accumulation time (Pearson and Eglinton 2000; Ohkouchi et al. 2003; Smittenberg et al. 2004; Mollenhauer et al. 2005; Mollenhauer and Eglinton 2007; Eglinton and Eglinton 2008; Vonk et al. 2014; Winterfeld et al. 2018; Berg et al. 2020; Bliedtner et al. 2020).

*Corresponding author. Email: bernhard.aichner@gmx.de

Compound-specific radiocarbon analysis (CSRA), i.e. analysis of radiocarbon (^{14}C) contents of specific biomarker compounds, can give information about their mean residence time in the respective compartment (Eglinton et al. 1996; Ingalls and Pearson 2005; Rethemeyer et al. 2013), which has mostly been applied for marine study sites (Pearson et al. 2001; Mollenhauer et al. 2003; Ohkouchi and Eglinton 2008; Kusch et al. 2010; Galy and Eglinton 2011; Schefuss et al. 2016).

Lacustrine systems (Uchikawa et al. 2008; Douglas et al. 2014; Gierga et al. 2016; Douglas et al. 2018; Aichner et al. 2018; Yamamoto et al. 2020; Freimuth et al. 2021) have been comparably less studied. Also here, ages of plant waxes from catchment soils range from several hundreds to thousands of years at both temperate and warm/humid study sites. Further, significant offsets between biomarker ages and conventional age models have been observed.

No such data so far exist for a cold and arid high altitude lake system. The main purpose of this study was to identify discrepancies between the ages of plant wax-derived long-chain *n*-alkanes and the conventional age model, which may result in misinterpretation of the biomarker records. The study was performed in Lake Karakul and its catchment, a well-studied lake system in the Pamirs, Tajikistan (Taft et al. 2014; Heinecke et al. 2017a, 2017b, 2018; Mischke et al. 2017; Aichner et al. 2019; Figure 1). The cold and arid conditions are assumed to result in low carbon turnover and biomarker fluxes to sediments, which may result in significantly higher *n*-alkane ages compared to the bulk sediment. We measured ^{14}C contents of long-chain *n*-alkanes in surface soils of the lake catchment and in the sediment cores. Hereby we aimed (1) to determine the ages of soil-derived *n*-alkanes, as a likely source of sedimentary biomarkers, and (2) to quantify potential offsets between the ages of *n*-alkanes and sediments, the latter estimated by means of accelerator mass spectrometry (AMS) ^{14}C dating of total organic carbon (TOC) and optically stimulated luminescence (OSL) dating.

MATERIAL AND METHODS

Study Site

Lake Karakul (approx. 39°N and 73°25′E) is a closed-basin lake in the eastern Pamirs, Tajikistan, located in an active extension basin within a graben structure (Strecker et al. 1995; Komatsu 2016). While the lake covers 388 km^2 at an altitude of 3915 m a.s.l., its catchment area extends over 4464 km^2 and reaches up to peaks at 6780 m a.s.l. (Figure 1a). The mean annual precipitation (MAP) within the shielded lower basin is <100 mm, but often exceeds 1000 mm at higher altitudes, mainly due to enhanced winter precipitation. Mean January, July and annual temperatures are −18.1, 8.5, and −4.0°C, respectively (Williams and Konovalov 2008).

The vegetation around the lake consists mainly of species from the Cyperaceae family. At wetter sites they form either dense saline meadows dominated by *Carex* and *Kobresia* species or saline marshes dominated by *Blysmus* species, the latter usually located close to the lake shore. Sites where soil moisture is lower are characterized by sparse vegetation with *Carex pseudofoetida*. At dry sites, species from the Cyperaceae family are replaced by plants adapted to dry and stony soils, such as *Krashenninikovia ceratoides*, *Artemisia pamirica* or *Ajania tibetica* (Safarov 2003; Mętrak et al. 2017, 2019).

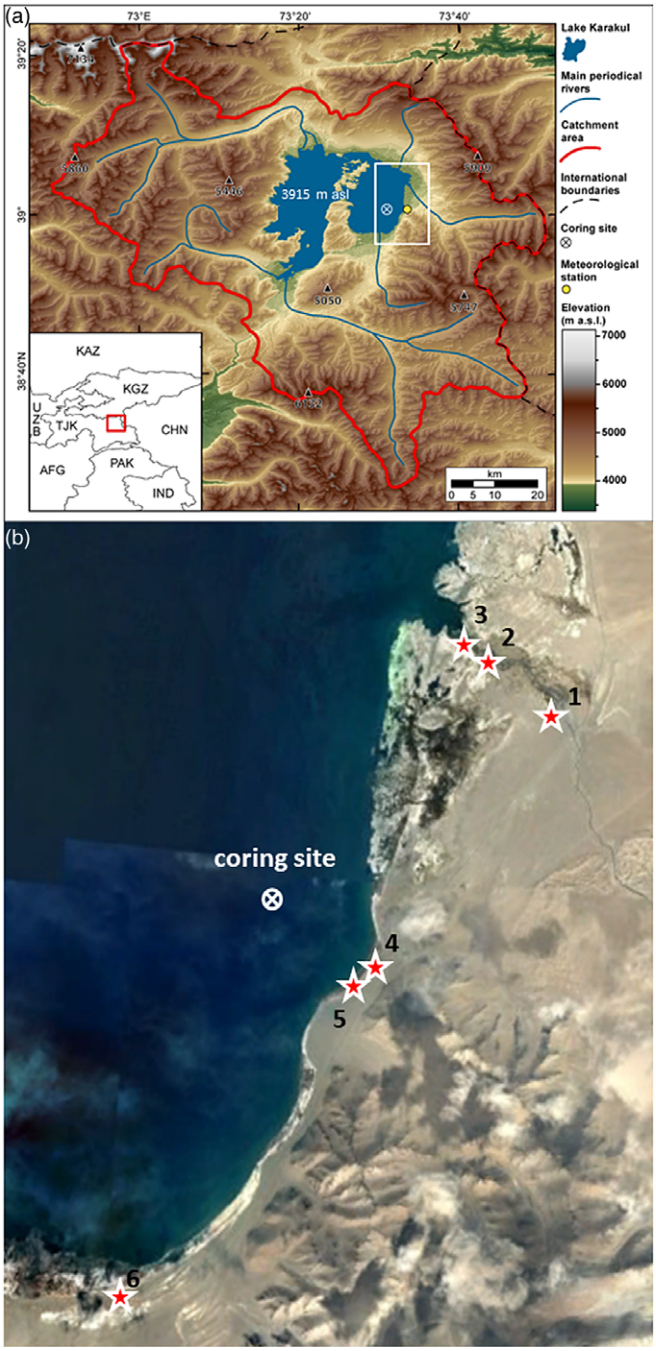

Figure 1 (a) Topographic map of Lake Karakul and its catchment, modified after Taft et al. (2014) with permission from *Springer Nature*; (b) locations of soil samples (red stars) and sediment core KK12-comp. (For color versions of all figures the reader is referred to the web version of this article.)

Since the year 2008, several sediment cores spanning the last ca. 4–31 ka BP were obtained from Lake Karakul and investigated by sedimentological, geochemical and biological analyses (Mischke et al. 2010, 2017; Taft et al. 2014; Heinecke et al. 2017a, 2017b, 2018; Aichner et al. 2019). The obtained results, and paleoshorelines 35 m above the present lake level, dating to 15 ka BP (Komatsu and Tsukamoto 2015), indicate past lake-level changes, which were mainly driven by changes in the seasonality of the precipitation-evaporation balance (Aichner et al. 2019).

Sampling

The collected soil samples were selected to represent the variety of soils in the catchment and hence cover multiple potential source material of the lake sediment. Pictures of sampling spots are provided in the Supplementary Figures S1. Soil samples #1–3 were collected along a stream that runs from the Sarikol Range on the border between Tajikistan and China and enters a small bay at the northeastern part of Karakul Lake (Figure 1b; Table 1). Sample #1, located farthest from the lake, was taken from an area covered with sparse vegetation typical for slightly moist places. A dominating species there is *Carex pseudofoetida* characterized by long creeping rhizomes. It is accompanied by *Rheum reticulatum* and species from genera *Potentilla* and *Kobresia*. Samples #2 and #3 were collected closer to the lake, with sample #3 placed within the stream delta. Both locations are covered by dense wetland vegetation (small sedge meadows) dominated by species belonging to Cyperaceae family (e.g., *Carex orbicularis, Carex microglochin, C. pseudofoetida, Eleocharis* sp.). Soil samples #4 and #5 were collected on the narrow beach south of Karakul village. The beach represents dense saline marshes dominated by *Blysmus rufus* and, in drier places, by *Carex microglochin*. All soil samples were collected as blocks of approximately 10 cm width, 10 cm length and 20 cm depth, cut with a serrated knife and packed separately into linen bags after removal of the surficial live vegetation layer and dense roots. Air-dried samples were crushed by hand, mixed thoroughly and sieved (1-mm mesh) to remove coarse matter and fine roots. Sample #6 was collected from a large alluvial plain close to the southern shore of Lake Karakul. Here, the top 0–10 cm of soil above a layer with increased inclusion of stones/gravel, were sampled.

For sediment samples, two sections of the sediment core KK12-1 (Heinecke et al. 2017a, 2017b; Mischke et al. 2017) were selected (Figure 2). Based on the concentrations of $n\mathrm{C}_{29}$- and $n\mathrm{C}_{31}$-alkanes (Aichner et al. 2019), the needed sediment amount for CSRA was estimated. Hence, one core section from 488–465 cm depth and another one from 695–669 cm depth were chosen, representing the middle Holocene (6792–5760 cal BP) and the Late Glacial (16,877–14,673 cal BP).

Age Model

Details of age modeling of the composite sediment core KK12-comp have been published previously (Mischke et al. 2017; Figure 2a). Briefly, this age model is based on AMS ^{14}C ages of TOC and OSL dates and was computed with OxCal 4.2, using IntCal13 (Bronk Ramsey and Lee 2013; Reimer et al. 2013). Two parallel cores (KK12-1 and KK12-2) were correlated by means of elemental data derived from XRF scanning at 2-mm resolution. Samples for ^{14}C dating of TOC were taken from both parallel cores. Resulting ^{14}C ages were corrected for a lake-reservoir effect of 1368 yr before calibration. The lake-reservoir (LRE) effect was estimated by using average ages determined on material of two living

Table 1 Description of analyzed soil and sediment core samples.

Sample name	Sampling depth (cm)	Dry weight (g)	Latitude (°N)	Longitude (°E)	Comment
Soil 1	0–20	35.7	39.04895	73.58900	Sparse vegetation with *C. pseudofoetida*
Soil 2	0–20	42.7	39.05611	73.57407	Small sedge meadow/alluvial plain
Soil 3	0–20	48.1	39.05894	73.56903	Small sedge meadow/alluvial plain
Soil 4	0–20	42.0	39.00631	73.55369	Saline marsh; sulfur rich
Soil 5	0–20	49.3	39.00393	73.55179	Saline marsh; sulfur rich
Soil 6	0–10	278.0	38.95272	73.50949	Grassland/alluvial plain
Core A	465–488	57.3	39.01760	73.53270	ca. 6.8–5.8 ka cal BP
Core B	669–695	88.2	39.01760	73.53270	ca. 16.9–14.7 ka cal BP

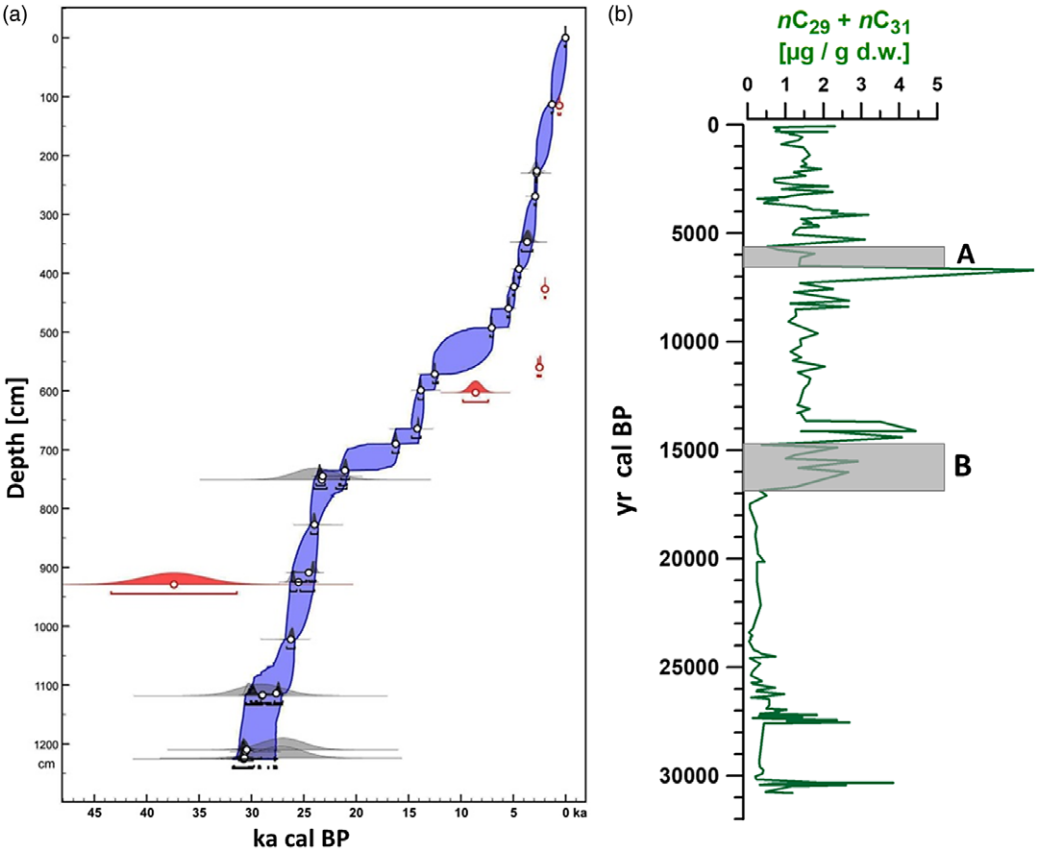

Figure 2 (a) Age model (2σ uncertainty range) of core KK12-comp, based on ^{14}C-TOC (black) and OSL dates (gray). Original calibrated ages shaded in light gray, modeled ages in dark gray. Five omitted ages in red. White dots and brackets mark µ and 2σ of the modeled ages (reused with permission from Elsevier from Mischke et al. 2017). (b) Concentrations of nC_{29}- and nC_{31}-alkanes in sediment core KK12-2 (Aichner et al. 2019). Gray shaded areas A and B indicate core sections that were extracted for CSRA.

aquatic plants, collected on the coring location (Mischke et al. 2017). Radiocarbon ages were complemented by OSL dating results from core KK12-2.

To allow comparison with this published TOC/OSL age model, ^{14}C ages of biomarkers as listed in Table 2 have been calibrated with OxCal using IntCal13 (Reimer et al. 2013), despite a newer version of IntCal that has been published in the meantime.

Sample Preparation

All sediment and soil samples were freeze-dried, homogenized and solvent extracted (ASE 350, Dionex, USA) with a mixture of dichloromethane and methanol (9:1 v/v) at 100°C and 75 bar for two cycles. Between 35 and 278 g of dry soil and 57 and 88 g of dry sediment were extracted per sample (Table 1). The aliphatic fraction containing *n*-alkanes was separated with silica gel chromatography (5 cm × 40 mm; pore size 60 Å, 230–400 mesh size, 40–63 µm particle size) with *n*-hexane. The aliphatic fraction of the sediment samples was further purified by removing unsaturated compounds with $AgNO_3$-coated silica gel. Individual *n*-alkanes were identified

Table 2 AMS ^{14}C results for *n*-alkanes from soil and sediment samples. The total amount of C (μg) obtained for analysis as determined on the vacuum line (soil #1, #2/3, #4/5) and by EA (soil #6, core A, B). Calibrated ages were computed with OxCal using IntCal13 (Reimer et al. 2013) and reported as mean ages (μ) with 1σ uncertainties.

Sample	Compounds	Lab ID	C (μg)	$F^{14}C$	+/–	Age (BP)	σ	Age (cal BP)	σ
Soil 1	C29 + C31	COL5657	24	0.718	0.009	2261	105	2278	155
Soil 2+3	C29 + C31	COL5658	71	0.848	0.004	1326	39	1250	39
Soil 4+5	C29 + C31	COL5659	51	0.794	0.008	1856	77	1785	92
Soil 6	C29	COL6138	19	1.024	0.013	>modern	102	124	79
Soil 6	C31	COL6139	16	0.977	0.013	185	109	207	129
Core A	C29	COL6132	28	0.454	0.010	6349	171	7232	183
Core A	C31	COL6133	12	0.459	0.012	6262	204	7134	220
Core B	C29	COL6134	17	0.161	0.009	14691	450	17575	573
Core B	C31	COL6135	7	0.271	0.012	10492	354	12202	470

and quantified relative to an external standard by gas chromatography (GC) using an Agilent 7890B system equipped with a flame ionization detector (FID).

Individual *n*-alkane homologs were isolated by repeated injection on a preparative gas chromatography system (prepGC). The prepGC consists of a 7690 Agilent GC (Agilent, USA) equipped with an ultralow bleed fused silica capillary column (30 m, film thickness 0.5 μm, 0.53 mm ID, RTX-1, RESTEK, USA), a CIS 4 injection system (Gerstel, Germany), and coupled to a preparative fraction collector (PFC, Gerstel, Germany). Individual *n*-alkanes were collected at room temperature in glass traps attached to the PFC and later flushed with 1 ml dichloromethane. Purity and amount of the isolated compounds were determined by GC-FID. Average recovery of target compounds after prepGC was 24% (Table S1).

In order to achieve quantities large enough for reliable ^{14}C dating of CO_2 using a gas ion source (Schiffer et al. 2019; Melchert et al. 2020), some of the individual compounds of the soil samples were combined as given in Table 2: For Soil #1 nC_{29}- and nC_{31}-alkanes were pooled, nC_{29}- and nC_{31}-alkanes from soil #2 and #3, as well as from soil #4 and #5 were combined to one sample respectively. For soil #6 and the sediment samples *n*-alkane homologues were dated individually. The nC_{27}-alkane was not considered for CSRA, as it was not possible to chromatographically separate this homologue from another unknown compound via prepGC. The samples were prepared in two batches at different times. While the isolation with prepGC remained the same, the preparation for ^{14}C analyses differed. The *n*-alkanes isolated from the soil samples #1, #2/3 and #4/5 were prepared by sealed tube combustion using the gas injection system (GIS) interface (Stolz et al. 2017), as described in Rethemeyer et al. (2019). In contrast, the *n*-alkanes purified from soil #6 and sediment core A, B were transferred into tin capsules to be analyzed via direct combustion in an elemental analyzer (EA) coupled with the GIS interface (Stolz et al. 2019).

Data Correction

In order to correct the results for possible contamination added during the purification procedure and to determine contributions of extraneous C, two standards of known ^{14}C

concentration were processed and dated. We used (1) squalane, a C_{30} isoprenoid with a modern ^{14}C signature (Fluka, PN 85629-50ml, Lot. 0001418796; $F^{14}C$ 1.0187 ± 0.0033) and (2) a C_{18} *n*-alkane (Fluka, PN 74691-5g, Lot. 0001448903, $F^{14}C < 0.0008$) free of ^{14}C, i.e. as a blank.

Since all samples were expected to be of similar size, two replicates of the modern standard and blank were measured along with the samples and the correction was performed as described in BATS (Wacker et al. 2010). Recoveries of the standards after prepGC accounted for ≈60%. The $F^{14}C$ values of the squalane and nC_{18} scattered by 1‰ and 20%, respectively. The $\delta^{13}C$ values scattered by 1.4‰ and 0.2‰. The reported errors include the Poisson errors of the AMS measurements of the standards and of the individual samples. However, according to the model of constant contamination as described in Hanke et al. (2017), an additional error is expected that comes from the measurement uncertainties of the sample masses, which are proportionally larger for smaller sample amounts. The most extreme influence is therefore expected for the sample COL6135 (7 µg), which in fact shows a relatively high deviation of the analyzed isotope ratios of about 70%. With the measured blank values, the constant contamination is estimated to be about 2 µg, assuming a $F^{14}C$ value of the contaminant of 0.4.

RESULTS

Except for sample #1, which shows larger relative amounts of nC_{27}-alkane, all soil samples are characterized by a pronounced dominance of nC_{29}- and nC_{31} alkanes. The absolute amounts of extracted *n*-alkanes range from 13 to 231 µg before and from 5 to 23 µg after prepGC, (Table S1). The $F^{14}C$ values for the soil samples, which are based on either pooled or individual compounds, range from 0.718 to 1.024, equivalent to conventional ^{14}C ages ranging from 2261 ± 105 BP to modern (–187 ± 102 BP) (Table 2).

The sediment samples exhibit *n*-alkane amounts from 62 to 92 µg before and 4 to 22 µg after prepGC (Table S1). In core sample A, the $F^{14}C$ values are 0.454 ± 0.010 (nC_{29}) and 0.459 ± 0.012 (nC_{31}), while in core sample B the results span from 0.161 ± 0.009 (nC_{29}) to 0.271 ± 0.012 (nC_{31}). The values correspond to conventional ages of 6349 ± 171 (nC_{29}) and 6262 ± 204 (nC_{31}) BP (sample A), as well as 14,691 ± 450 (nC_{29}) and 10,492 ± 354 (nC_{31}) BP (sample B) (Table 2).

DISCUSSION

Variability of n-alkane Ages in Surface Soils

The mean residence times of soil organic matter is believed to be relatively short, i.e., a few decades (Kögel-Knabner and Amelung 2014; Feng et al. 2016). However, a number of studies identified a significantly older carbon pool, i.e., several hundreds to a few thousands of years old, which may consist of more recalcitrant or physically stabilized compounds (Schöning and Kögel-Knabner 2006; Smittenberg et al. 2006; Trumbore 2009; Douglas et al. 2014, 2018; Van der Voort et al. 2017).

In the Karakul catchment, surface soils were sampled along a transect from sites covered with sparse vegetation not affected by rivers/streams in the catchment (#1), via soils covered with sedge meadows developed on the alluvial plains of rivers and creeks (pooled sample #2/#3 and sample #6), to samples from the saline marshes in the vicinity to the shore of Lake Karakul

(pooled sample #4/#5) (Figure 1). The highest calibrated age of all dated compounds (2278 ± 155 cal BP) was measured in sample #1 (Table 2). The *n*-alkanes in the pooled saline marsh samples #4/#5 exhibit the second oldest age (1785 ± 92 cal BP). Alluvial samples show mixed results, but principally the lowest ages ranging from modern in #6, to 1250 ± 39 cal BP in the pooled samples #2/#3.

Thus, there is a tendency towards higher *n*-alkane ages in the surface soils with lowest influence of river water. We hypothesize that there are three major reasons behind this observation: (I) different exposure to ground and surface water and hence proneness to surface erosion and translocation of organic matter (OM). Precipitation amounts in the lower parts Karakul basin are low but significantly higher at higher altitudes. This leads to a strong increase of riverine discharge during the spring/early summer snow melt and large alluvial plains, such as around sampling spot #6, are partially flooded. From soils located in such alluviums or closer to rivers, mobilization and removal of OM is probably efficient and faster. In the saline mashes (spots #4/#5) OM might be protected from translocation due to dense vegetation cover, which could explain the relatively old biomarker age in the sample from those locations.

A second major cause may be (II) different production rates of biomass at wet sites compared to dry sites. We suggest that river flooding delivers nutrients to the soil and supports faster plant growth, resulting in larger inputs of fresh OM and hence a younger organic carbon (OC) pool. Regions further away from rivers are most likely areas of lower OM input and slower OC cyling because they are drier and vegetation is more sparse.

Another possible factor of relevance (III) is the degree of inclusion of deeper soil layers. Sub-recent and older OM is more likely included in the C pool beneath the uppermost soil layer (Douglas et al. 2014). Therefore, at spot #6, the smaller sampling depth of 0–10 cm could partly explain the youngest ages of the biomarkers, compared to the other sites where sampling depths were 0–20 cm. The saline marshes (spots #4/#5) are characterized by a gray and loamy B-horizon, located under a thin carpet of living roots, i.e., the contribution of sub-recent OM to the sample might be relatively large.

The variable ages of soils in the lake catchment give evidence for varying accumulation and translocation dynamics of organic biomarkers in the Karakul catchment. This is important in context of the question which kind of material is preferentially transported to the lake and deposited in sedimentary sequences. The data suggest that locations under riverine and lake water influence are less prone to accumulation of OM over longer time-scales. Accelerated and increased riverine discharge after snowmelt could facilitate erosion of topsoils at those spots. Therefore they are more likely originators of biomarkers deposited as part of the lake sediments. In contrast, plant waxes from the sparse alpine meadows, which are mainly precipitation fed, are less prone to be transported to the lake.

In addition to surface water, eolian transport cannot be ruled out as an additional factor for translocation of leaf waxes to the lake. Long range transport has been shown to be an important source of dust in Central Asian mountains (Wu et al. 2009, 2015; Mętrak et al. 2019). It is unclear whether this is relevant for our study area due to the shielded nature of the Karakul basin. Locally, strong winds connected to the mountain-lake system, could at least facilitate short range transport of leaf waxes—either directly from the leaf surfaces or indirectly via dust particles derived from dry soils.

Age Discrepancies of n-alkanes and Sediments

The radiocarbon ages of the sedimentary nC_{29}- and nC_{31}-alkanes were compared with the published age model, which is based on TOC/OSL ages, of the respective sediment core (Figure 3). Relatively large sections of the core had to be extracted to obtain sufficient concentrations of the long-chain *n*-alkanes for CSRA, i.e., 23 cm for sample A and 26 cm for sample B (Figure 3). As a consequence, the respective core sections cover relatively wide age ranges of ca. 1000 years (6792–5760 cal BP) for sample A, and ca. 2200 years (16,877–14,673 cal BP) for sample B. Taking the 1σ-uncertainty intervals into account, these ranges significantly increase to ca. 2000 years (i.e., 7254–5274 cal BP; sample A) and >4100 years (18,036–13,911 cal BP; sample B), respectively.

^{14}C dating of sediments of lakes on the Tibetan Plateau is often complicated by a significant LRE (hard water effect), which might change over time (Lee et al. 2011; Hou et al. 2012; Zhang et al. 2012; Mischke et al. 2013; Lei et al. 2014; Haberzettl et al. 2015; Xu et al. 2021). Hence, if dating of terrestrial plant remains is not possible, radiocarbon dating of bulk TOC might generate wrong age estimates. In case of the sediment core KK12-comp from Lake Karakul, it was attempted to achieve better age control by including OSL ages. In six of total ten cases, OSL dates corresponded well with ^{14}C dates of TOC (Figure 2a; Mischke et al. 2017), suggesting a relatively constant LRE throughout the core. However, offsets of ca. 5000 years between the two dating methods occurred around 600 cm depth (Figure 3b). Based on a general outlier model run with 5% probability in OxCal (Bronk Ramsey 2009), the respective OSL date of 8600 ± 600 yr BP was considered as outlier and hence omitted in favor of two ^{14}C-TOC dates from 570 and 600 cm depth (Figure 3b; Mischke et al. 2017).

In three of four cases the calibrated ages of individual *n*-alkanes fall close to the lowest end of the 1σ-uncertainty interval of the TOC/OSL-age model:

For core sample A, the ages of both measured *n*-alkanes are similar (nC_{29}: 7232 ± 183 cal BP; nC_{31}: 7134 ± 220 cal BP), taking their age uncertainties into account (Figure 3a). This is despite the fact that on average 2–3‰ higher $\delta^{13}C$ values of nC_{29} in contrast to nC_{31} provide evidence for partially different sources of these compounds (Figure 3a; Aichner et al. 2019). Higher $\delta^{13}C$ values can be explained by contribution of aquatic macrophytes to the sedimentary nC_{29}-alkane pool, which has been frequently observed in high altitude lakes of the Tibetan Plateau (Aichner et al. 2010; Liu et al. 2015) and recently also in a temperate lake system (Andrae et al. 2020). In case of Lake Karakul, macrophytes dominated organic compounds in the middle to late Holocene (Aichner et al. 2019). A partial contribution of macrophytes to the nC_{29} pool in core section A is therefore plausible.

The two *n*-alkanes in sample A are ca. 1000 years older than the average TOC/OSL age (dashed black line in Figure 3a) of the extracted core section. This age difference could indeed be evidence for a delayed sedimentation of terrestrial compounds, due to transport processes and/or "pre-aging" as a relevant factor, indicated by ages of soil *n*-alkanes. On the other hand, ages of sedimentary *n*-alkanes are still within the 1σ-uncertainty range of the conventional age model, which excludes a definite statement about such processes.

Similarly, in core sample B, the age of the nC_{29}-alkane (17575 ± 573 cal BP) falls close to the lower end but lies still within the 1σ-uncertainty range of the conventional age model. In this case, the nC_{29}-alkane is ca. 1900 years older than the average age based on the TOC/OSL-age

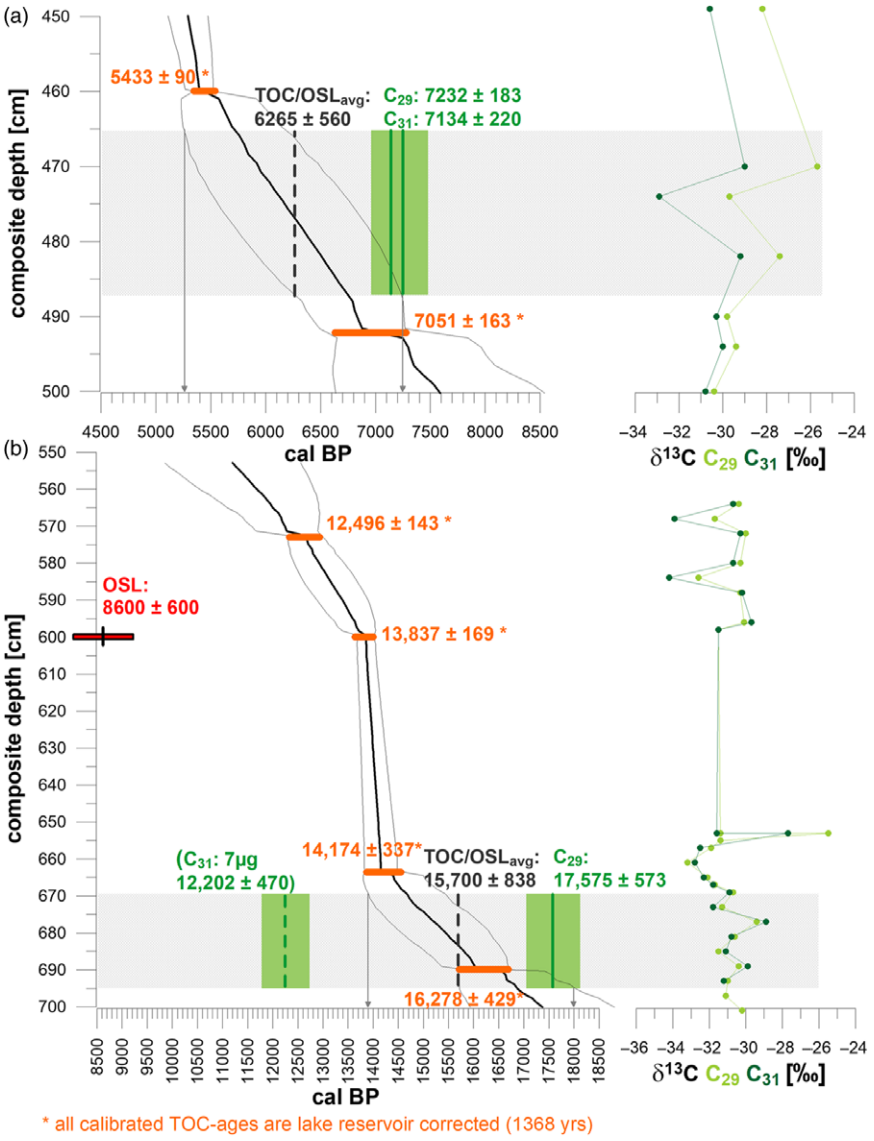

Figure 3 µ and 1σ uncertainty of calibrated radiocarbon ages of nC$_{29}$- and nC$_{31}$-alkanes (green) in the sediment core sections A (top) and B (bottom) in comparison to the age model (black line: median ages; gray line: 1σ uncertainty) based on sedimentary TOC (orange) and on OSL ages (red). To maintain consistency with the published age model (Mischke et al. 2017), all biomarker ages were calibrated with IntCal13 (Reimer et al. 2013). Gray-shaded interval on the depth-axes indicate the core section extracted for CSRA. Arrows towards the x-axes mark the extents of the 1σ-range of the extracted core sections. The vertical dashed black line indicates the average age of the extracted core section based on the published age model (TOC/OSL$_{avg}$). Right panels display δ^{13}C values of nC$_{29}$ and nC$_{31}$ alkanes.

model (Figure 3b). In contrast, the nC$_{31}$-alkane exhibits a significant age offset (12202 ± 470 cal BP), with an age ca. 5300 years younger than that of nC$_{29}$, i.e., far off the conventional age model.

The two possible explanations for the large offset of the nC_{31}-alkane age are (I) different sources of the two compounds and overestimation of ages of the conventional age model; or (II) analytical reasons.

Possibility (I) is only plausible with the younger age of nC_{31} reflecting the true timing of sedimentation. This would imply significant pre-aging of nC_{29} and a conventional age model that provides too old ages for the respective core section. Assuming that the outlier OSL date at 600 cm more precisely reflects the timing of sediment accumulation, the modeled ages in the respective core section would be too old. Similarly, also the modeled ages in the section sampled for CSRA, which are constrained by two ^{14}C dates of TOC, could be overestimated. However, different sources of nC_{29} and nC_{31} in the sedimentary pool are unlikely due to the sparse vegetation in the catchment and generally similar $\delta^{13}C$ values of the two compounds in the respective core section (Figure 3b). An aquatic contribution to nC_{29} during the Late Glacial can also be excluded (Aichner et al. 2019). Therefore, if the TOC/OSL-age model is not correct, we would expect similar offsets for both dated *n*-alkanes. For these reasons we consider possibility (I) as unlikely.

Possibility (II) for the age offset is that the age of nC_{31} encompasses larger uncertainty because of analytical reasons. Sample size, i.e., the amount of isolated C after prepGC, is crucial for CSRA (Gierga et al. 2016). The nC_{31} isolated from sample B exhibited by far the lowest amount of datable material (7µg C; Table 2). It is therefore the sample most susceptible for contamination with material containing a modern ^{14}C-signature. In addition, the smaller the sample size, the higher is the potential proportion of contamination, which is unaffected by the applied data calibration and correction strategies. For these reasons, we consider analytical bias due to low amounts of C to be the most likely cause for the age offset between the two *n*-alkanes in core sample B.

Overall, the mean residence times of *n*-alkanes, i.e., the offsets of 1000–1900 years between the TOC/OSL-age model and the ages of *n*-alkanes, are larger than in most previous studies from lacustrine systems (Uchikawa et al. 2008; Douglas et al. 2014, 2018; Gierga et al. 2016; Yamamoto et al. 2020; Freimuth et al. 2021). On the other hand, they are in range of average ages as determined in soils from the Karakul catchment. This speaks for either a mixed origin of compounds, i.e., from multiple sites characterized by variable pre-aging, or for sources mainly from spots with young to intermediate ages of biomarkers, such as the alluvial plains under riverine influence (samples #2/#3 and #6). An explanation for higher offsets in the glacial period (sample B) is higher soil erosion induced by increased summer humidity in the Late Glacial (from ca. 17 to 14 ka BP; Aichner et al. 2019), which could have led to mobilization of older OM that has been stored in soils during the glacial.

CONCLUSIONS

Three of four dated compounds in two sediment core samples are 1000–1900 years older than average sediment ages modeled by means of ^{14}C-TOC and OSL dates. On the other hand, these plant wax ages still fall within the lowermost margins of the age models 1σ-uncertainty ranges, which do not yet include additional factors such as changes of LRE.

Based on ages of biomarkers extracted from soil samples, we hypothesize that sedimentary biomarkers are most likely originated from spots with short to intermediate turnover time of organic matter. These are for example the alluvial plains close to the southern and

eastern shores and comparable spots with relatively short transport paths and times via surface runoff.

Overall, the data suggest that terrestrial *n*-alkanes are potentially older than the TOC/OSL-based age model indicates. However, in context of the relatively large uncertainties of such age models, the offsets to plant wax ages appear moderate. We therefore conclude that conventional age models can be potentially applied to terrestrial biomarkers, but care must be taken especially when interpreting such proxy data with respect to short-term events.

ACKNOWLEDGMENTS

We acknowledge the German Science Foundation (DFG project Ai 134/2-2) and the Polish National Science Centre (Grant No 2013/09/B/ST10/01662) for funding. We thank Muzaffar Shodmonov, Foteh Rahimov and Yakub Shoev (Tajik Hydromet) for logistical support during fieldwork in 2018. Assistance in the field was provided by Grzegorz Górecki, Natalia Khomutovska, and Anne Köhler. Marcin Sulwiński, PhD is acknowledged for help with identification of plant species. We are further grateful to Bianca Stapper and Sonja Berg for help with compound-specific radiocarbon measurements. The constructive comments of two anonymous reviewers helped to significantly improve the manuscript.

SUPPLEMENTARY MATERIAL

To view supplementary material for this article, please visit https://doi.org/10.1017/RDC.2021.78

REFERENCES

Aichner B, Herzschuh U, Wilkes H. 2010. Influence of aquatic macrophytes on stable carbon isotope signatures of sedimentary organic matter in lakes on the Tibetan Plateau. Organic Geochemistry 41:706–718.

Aichner B., Makhmudov Z, Rajabov I, Zhang Q, Pausata FSR, Werner M, Heinecke L, Kuessner M, Feakins S, Sachse D, Mischke S. 2019. Hydroclimate in the Pamirs was driven by changes in precipitation-evaporation seasonality since the last glacial period. Geophysical Research Letters 46: 2019GL085202. doi: 10.1029/2019GL085202.

Aichner B, Ott F, Słowiński M, Noryśkiewicz AM, Brauer A, Sachse D. 2018. Leaf wax n-alkane distributions record ecological changes during the Younger Dryas at Trzechowskie paleolake (northern Poland) without temporal delay. Climate of the Past 14:1607–1624. doi: 10.5194/cp-14-1607-2018.

Andrae JW, McInerney FA, Kale Sniderman JM. 2020. Carbon isotope systematics of leaf wax n-alkanes in a temperate lacustrine depositional environment. Organic Geochemistry 150:104121.

Berg S, Jivcov S, Kusch S, Kuhn G, Wacker L, Rethemeyer J. 2020. Compound-specific radiocarbon analysis of (Sub-)Antarctic coastal marine sediments—potential and challenges for chronologies. Paleoceanography and Paleoclimatology 35:2020PA003890.

Bliedtner M, von Suchodoletz H, Schäfer I, Welte C, Salazar G, Szidat S, Haas M, Dubois N, Zech R. 2020. Age and origin of leaf wax n-alkanes in fluvial sediment–paleosol sequences and implications for paleoenvironmental reconstructions. Hydrology and Earth System Sciences 24:2105–2120. doi: 10.5194/hess-24-2105-2020.

Bronk Ramsey C. 2009. Dealing with outliers and offsets in radiocarbon dating. Radiocarbon 51:1023–1045.

Bronk Ramsey C, Lee S. 2013. Recent and planned developments of the program OxCal. Radiocarbon 55: 720–730.

Castañeda IS, Schouten SA. 2011. Review of molecular organic proxies for examining modern and ancient lacustrine environments. Quaternary Science Reviews 30:2851–2891.

Douglas PMJ, Pagani M, Eglinton TI, Brenner M, Hodell DA, Curtis JH, Ma KF, Breckenridge A. 2014. Pre-aged plant waxes in tropical lake sediments and their influence on the chronology of molecular paleoclimate proxy records. Geochimica et. Cosmochimica Acta 141:346–364.

Douglas PMJ, Pagani M, Eglinton TI, Brenner M, Curtis JH, Breckenridge A, Johnston K. 2018. A long-term decrease in the persistence of soil carbon caused by ancient Maya land use. Nature Geoscience 5:645–649. doi: 10.1038/s41561-018-0192-7.

Eglinton G, Hamilton RJ. 1967. Leaf epicuticular waxes. Science 156(3780):1322–1335.

Eglinton TI, Aluwihare LI, Bauer JE, Druffel ERM, McNichol AP. 1996. Gas chromatographic isolation of individual compounds from complex matrices for radiocarbon dating. Analytical Chemistry 68:904–912.

Eglinton TI, Benitez-Nelson B, Pearson A, McNichol AP, Bauer JE, Druffel ERM. 1997. Variability in radiocarbon ages of individual organic compounds from marine sediments. Science 277:796–799

Eglinton TI, Eglinton G. 2008. Molecular proxies for paleoclimatology. Earth and Planetary Science Letters 275(1–2):1–16. doi: 10.1016/j.epsl.2008.07.012.

Feng, W, Shi Z, Jiang J, Xia J, Liang, J, Zhou J. 2016. Methodological uncertainty in estimating carbon turnover times of soil fractions. Soil Biology and Biochemistry 100:118–124. doi: 10.1016/j.soilbio.2016.06.003.

Freimuth EJ, Diefendorf AF, Lowell TV, Schartman AK, Landis JD, Stewart AK, Bates BR. 2021. Centennial-scale age offsets of plant wax n-alkanes in Adirondack lake sediments. Geochimica et Cosmochimica Acta 300:119–136. doi: 10.1016/j.gca.2021.02.022.

Galy V., Eglinton T. 2011. Protracted storage of biospheric carbon in the Ganges–Brahmaputra basin. Nature Geoscience 4:843–847. doi: 10.1038/ngeo1293.

Gierga M, Hajdas, I, van Raden UJ, Gilli A, Wacker L, Sturm M, Bernasconi SM, Smittenberg RH. 2016. Long-stored soil carbon released by prehistoric land use:Evidence from compound-specific radiocarbon analysis on Soppensee lake sediments. Quaternary Science Reviews 144, 123–131. doi: 10.1016/j.quascirev.2016.05.011.

Haberzettl T, Henkel K, Kasper T, Ahlborn M, Su Y, Wang J, Appel E, St-Onge G, Stoner J, Daut G, Zhu L, Mäusbacher R. 2015. Independently dated paleomagnetic secular variation records from the Tibetan Plateau. Earth and Planetary Science Letters 416:98–108.

Hanke UM, Wacker L, Haghipour N, Schmidt MWI, Eglinton TI, McIntyre CP. 2017. Comprehensive radiocarbon analysis of benzene polycarboxylic acids (BPCAs) derived from pyrogenic carbon in environmental samples. Radiocarbon 59(4):1103–1116. doi: 10.1017/RDC.2017.44.

Heinecke L, Epp LS, Reschke M, Stoof-Leichsenring KR, Mischke S, Plessen B, Herzschuh U. 2017a. Aquatic macrophyte dynamics in Lake Karakul (Eastern Pamir) over the last 29 cal ka revealed by sedimentary ancient DNA and geochemical analyses of macrofossil remains. Journal of Paleolimnology 58:403–417.

Heinecke L, Fletcher WJ, Mischke S, Tian F, Herzschuh U. 2018. Vegetation change in the eastern Pamir Mountains, Tajikistan, inferred from Lake Karakul pollen spectra of the last 28 kyr. Palaeogeography, Palaeoclimatology, Palaeoecology 511:232–242.

Heinecke L, Mischke S, Adler K, Barth A, Biskaborn BK, Plessen B, Nitze I, Kuhn G, Rajabov I, Herzschuh U. 2017b. Climatic and limnological changes at Lake Karakul (Tajikistan) during the last 29 cal ka. Journal of Paleolimnology 58(3):317–334.

Hou J, D'Andrea WJ, Liu Z. 2012. The influence of ^{14}C reservoir age on interpretation of paleolimnological records from the Tibetan Plateau. Quaternary Science Reviews 48:67–79.

Ingalls AE, Pearson A. 2005. Ten years of compound-specific radiocarbon analysis. Oceanography 18:18–31. doi: 10.5670/oceanog.2005.22.

Kögel-Knaber I, Amelung W. 2014. Dynamics, chemistry, and preservation of organic matter in soils. In: Holland HD, Turekian KK, editors. Treatise on geochemistry. 2nd edition, vol. 12. Oxford: Elsevier. ISBN 9780080959757. p. 157–215.

Komatsu T. 2016. Geomorphic features of the Eastern Pamirs, with a focus on the occurrence of intermontane basins. In: Kreutzmann H, Watanabe T, editors. Mapping transition in the Pamirs. Advances in Asian Human-Environmental Research. Springer. doi: 10.1007/978-3-319-23198-3_4.

Komatsu T, Tsukamoto S. 2015. Late Glacial lake-level changes in the Lake Karakul Basin (a closed Glacierized-Basin), eastern Pamirs, Tajikistan. Quaternary Research 83(1):137–149.

Kusch S, Rethemeyer J, Schefuß E, Mollenhauer G. 2010. Controls on the age of vascular plant biomarkers in Black Sea sediments, Geochimica et Cosmochimica Acta 74:7031–7047.

Lee MK, Lee YI, Lim HS, Lee JI, Choi JH, Yoon HI. 2011. Comparison of radiocarbon and OSL dating methods for a Late Quaternary sediment core from Lake Ulaan, Mongolia. Journal of Paleolimnology 45:127–135.

Lei Y, Tian L, Bird BW, Hou J, Ding L, Oimahmadov I, Gaodev M. 2014. A 2540-year record of moisture variations derived from lacustrine sediment (Sasikul Lake) on the Pamir Plateau. The Holocene 24:761–770. doi: 10.1177/095968361453443.

Liu W, Yang H, Wang H, An Z, Wang Z, Leng Q. 2015. Carbon isotope composition of long chain leaf wax n-alkanes in lake sediments:a dual indicator of paleoenvironment in the Qinghai-Tibet Plateau. Organic Geochemistry 83–84:190–201.

Melchert JO, Stolz A, Dewald A, Gierga M, Wischhöfer P, Rethemeyer J. 2020. Exploring

sample size limits of AMS gas ion source ^{14}C analysis at CologneAMS. Radiocarbon 61:1785–1793.

Mętrak M, Chachulski Ł, Navruzshoev D, Pawlikowski P, Rojan E, Sulwiński M, Suska-Malawska M. 2017. Nature's patchwork: How water sources and soil salinity determine the distribution and structure of halophytic plant communities in arid environments of the Eastern Pamir. PLoS One 12(3):e0174496.

Mętrak M, Szwarczewski P, Bińka K, Rojan E, Karasiński J, Górecki G, Suska-Malawska M. 2019. Late Holocene development of Lake Rangkul (Eastern Pamir, Tajikistan) and its response to regional climatic changes. Palaeogeography, Palaeoclimatology, Palaeoecology 521:99–113.

Mischke S, Weynell M, Zhang C, Wiechert U. 2013. Spatial variability of ^{14}C reservoir effects in Tibetan Plateau lakes. Quaternary International 313:147–155.

Mischke S, Rajabov I, Mustaeva N, Zhang C, Herzschuh U, Boomer I, Brown ET, Anderson N, Myrbo A, Ito E, Schudack ME. 2010. Modern hydrology and late Holocene history of Lake Karakul, eastern Pamirs (Tajikistan): a reconnaissance study. Palaeogeography, Palaeoclimatology, Palaeoecology 289:10–24.

Mischke S, Lai Z, Aichner B, Heinecke L, Mahmoudov Z, Kuessner M, Herzschuh U. 2017. Radiocarbon and optically stimulated luminescence dating of sediments from Lake Karakul, Tajikistan. Quaternary Geochronology 41:51–61.

Mollenhauer G, Eglinton TI, Ohkouchi N, Schneider RR, Müller PJ, Grootes PM, Rullkötter J. 2003. Asynchronous alkenone and foraminifera records from the Benguela Upwelling System. Geochimica et Cosmochimica Acta 67(12):2157–2171.

Mollenhauer G, Kienast M, Lamy F, Meggers H, Schneider RR, Hayes JM, Eglinton TI. 2005. An evaluation of 14C age relationships between co-oc-curring foraminifera, alkenones, and total organic carbon in continental margin sediments. Paleoceanography 20:2004PA001103.

Mollenhauer G, Eglinton, TI. 2007. Diagenetic and sedimentological controls on the composition of organic matter preserved in California Borderland Basin sediments. Limnology and Oceangraphy 52:558–576.

Ohkouchi N, Eglinton TI. 2008. Compound specific radiocarbon dating of Ross Sea sediments: a prospect for constructing chronologies in high-latitude oceanic sediments. Quaternary Geochronology 3:235–243.

Ohkouchi N, Eglinton TI, Hayes JM. 2003. Radiocarbon dating of individual fatty acids as a tool for refining Antarctic margin sediment chronologies. Radiocarbon 45:17–24.

Pearson A, Eglinton TI. 2000. The origin of n-alkanes in Santa Monica Basin surface sediment: a model based on compound-specific ^{14}C and ^{13}C data. Organic Geochemistry 31:1103–1116.

Pearson A, McNichol AP, Benitez-Nelson BC, Hayes JM, Eglinton TI. 2001. Origins of lipid biomarkers in Santa Monica Basin surface sediment:A case study using compound-specific ^{14}C analysis. Geochimica et Cosmochimica Acta 65(18):3123–3137.

Reimer PJ, Bard E, Bayliss A, Beck JW, Blackwell PG, Bronk Ramsey C, Buck CE, Cheng H, Edwards RL, Friedrich M, Grootes PM, Guilderson TP, Haflidason H, Hajdas I, Hatte C, Heaton TJ, Hoffmann DL, Hughen KA, Kaiser KF, Kromer B, Manning SW, Niu M, Reimer RW, Richards DA, Scott EM, Southon JR, Staff RA, Turney CSM, van der Plicht J, Hogg A. 2013. IntCal13 and Marine13 radiocarbon age calibration curves 0–50,000 years cal BP. Radiocarbon 55:1869–1887.

Rethemeyer J, Gierga M, Heinze S, Stolz A, Wotte A, Wischhöfer P, Berg S, Melchert JO, Dewald A. 2019. Current sample preparation and analytical capabilities of the radiocarbon laboratory at CologneAMS. Radiocarbon 61(5):1–12.

Rethemeyer J, Dewald A, Fülöp R, Hajdas I, Höfle S, Patt U, Stapper B, Wacker L. 2013. Status report on sample preparation facilities for ^{14}C analysis at the new CologneAMS centre. Nuclear Instruments and Methods in Physics Research B 294:168–172.

Safarov N. 2003. First National Report on Biodiversity Conservation [www document]. National Biodiversity and Biosafety Center, Dushanbe, p19. URL: https://www.cbd.int/doc/world/tj/tj-nr-01-p01-en.pdf.

Schefuß E, Eglinton TI, Spencer-Jones CL, Rullkötter J, De Pol-Holz R, Talbot HM, Grootes PM, Schneider RR. 2016. Hydrologic control of carbon cycling and ages carbon discharge in the Congo River basin. Nature Geoscience 9:687–690.

Schiffer M, Stolz A, López D, Spanier R, Herb S, Müller-Gatermann C, Heinze S, Binnie S, Melchert J, Kivel N, Schumann D, Rethemeyer J, Dunai T, Dewald A. 2019. Method developments for accelerator mass spectrometry at CologneAMS, $^{53}Mn/^{3}He$ burial dating and ultra-small $^{14}CO_2$ samples. Global and Planetary Change 184:103053. doi: 10.1016/j.gloplacha.2019.103053.

Schöning I, Kögel-Knabner I. 2006. Chemical composition of young and old carbon pools throughout Cambisol and Luvisol profiles under forests. Soil Biology and Biochemistry 38:2411–2424. doi: 10.1016/j.soilbio.2006.03.005.

Smittenberg RH, Hopmans EC, Schouten S, Hayes JM, Eglinton TI, Sinninghe Damsté JS. 2004. Compound-specific radiocarbon dating of the

varved Holocene sedimentary record of Saanich Inlet, Canada. Paleoceanography 19, PA2012. doi: 10.1029/2003PA000927.

Smittenberg RH, Eglinton, TI, Schouten S, Sinninghe Damsté JSS. 2006. Ongoing buildup of refractory organic carbon in boreal soils during the Holocene. Science 314:1283–1286. doi: 10.1126/science.1129376.

Stolz A, Dewald A, Altenkirch R, Herb S, Heinze S, Schiffer M, Feuerstein C, Müller-Gatermann C, Wotte A, Rethemeyer J, Dunai T. 2017. Radiocarbon measurements of small gaseous samples at CologneAMS. Nuclear Instruments and Methods in Physics Research Section B: Beam Interactions with Materials and Atoms 406(Part A):283–286. doi: 10.1016/j.nimb.2017.03.031.

Stolz A, Dewald A, Heinze S, Altenkirch R, Hackenberg G, Herba S, Müller-Gatermann C, Schiffer M, Zitzer G, Wotte A, Rethemeyer J, Dunai T. 2019. Improvements in the measurement of small $^{14}CO_2$ samples at CologneAMS. Nuclear Instruments and Methods in Physics Research. Section B: Beam Interactions with Materials and Atoms 439:70–75.

Strecker MR, Frisch W, Hamburger MW, Ratschbacher L, Semiletkin S, Samoruyev A, Sturchio N 1995. Quaternary deformation in the eastern Pamirs, Tajikistan and Kyrgyzstan. Tectonics 14(5):1061–1079.

Taft L, Mischke S, Wiechert U, Leipe C, Rajabov I, Riedel F. 2014. Sclerochronological oxygen and carbon isotope ratios in Radix (Gastropoda) shells indicate changes of glacial meltwater flux and temperature since 4,200 cal yr BP at Lake Karakul, eastern Pamirs (Tajikistan). Journal of Paleolimnology 52:27–41.

Trumbore S. 2009. Radiocarbon and soil carbon dynamics. Annual Review of Earth and Planetary Sciences 37:47–66. doi: 10.1146/annurev.earth.36.031207.124300.

Uchikawa J, Popp BN, Schoonmaker JE, Xu L. 2008. Direct application of compound-specific radiocarbon analysis of leaf waxes to establish lacustrine sediment chronology. Journal of Paleolimnolology 39:43–60.

van der Voort TS, Zell CI, Hagedorn F, Feng X, McIntyre CP, Haghipour N, Graf Pannatier E, Eglinton TI. 2017. Diverse soil carbon dynamics expressed at the molecular level. Geophysical Research Letters 44(23):11840–11850. doi: 10.1002/2017GL076188.

Vonk JE, Semiletov IP, Dudarev OV, Eglinton TI, Andersson A, Shakhova N. Charkim An, Heim B, Gustafsson Örjan. 2014. Preferential burial of permafrost-derived organic carbon in Siberian-Arctic shelf waters. Journal of Geophysical Research Oceans 119:8410–8421. doi: 10.1002/2014JC010261.

Wacker L, Christl M, Synal HA. 2010. Bats: a new tool for AMS data reduction Nuclear Instruments and Methods in Physics Research. Section B: Beam Interactions with Materials and Atoms 268(7–8):979. doi: 10.1016/j.nimb.2009.10.078.

Williams MW, Konovalov VG. 2008. Central Asia Temperature and Precipitation Data, 1879-2003, Version 1. Boulder, Colorado USA. NSIDC: National Snow and Ice Data Center. https://doi.org/10.7265/N5NK3BZ8 [accessed:January 2021].

Winterfeld M, Mollenhauer G, Dummann W, Köhler P, Lembke-Jene L, Meyer VD, Hefer J, McIntire C, Wacker L, Kokfelt U, Tiedemann R. 2018. Deglacial mobilization of pre-aged terrestrial carbon from degrading permafrost. Nature Communications 9:3666. doi: 10.1038/s41467-018-06080-w.

Wu G, Zhang C, Zhang X, Xu T, Yan N, Gao S. 2015. The environmental implications for dust in high-alpine snow and ice cores in Asian mountains. Global and Planetary Change 124:22–29. doi: 10.1016/j.gloplacha.2014.11.007.

Wu G, Xu B, Zhang C, Gao S, Yao T. 2009. Geochemistry of dust aerosol over the Eastern Pamirs. Geochimica et Cosmochimica Acta 73(4):977–989.

Xu D, Lu H, Jin C, Gu Z, Zuo X, Dong Y, Wang C, Wang L, Li H, Yu Y, Jin Y, Wu N. 2021. Application of multiple dating techniques to the Holocene sediments of Angrenjin Co in the southern Tibetan Plateau. Quaternary Geochronology 62:101148.

Yamamoto S, Miyairi Y, Yokoyama Y, Suga H, Ogawa N, Ohkouchi N. 2020. Compound-Specific Radiocarbon Analysis of Organic Compounds from Mount Fuji Proximal Lake (Lake Kawaguchi) Sediment, Central Japan. Radiocarbon 62(2):439–451. doi: 10.1017/RDC.2019.158.

Zhang JF, Liu, CL, Wu XH, Liu KX, Zhou LP. 2012. Optically stimulated luminescence and radiocarbon dating of sediments from Lop Nur (Lop Nor), China. Quaternary Geochronology 10:150–155.